ISSN 1070-3632, Russian Journal of General Chemistry, 2013, Vol. 83, No. 9, pp. 1635–1639. © Pleiades Publishing, Ltd., 2013.
Original Russian Text © V.P. Tolstoi, L.B. Gulina, 2013, published in Zhurnal Obshchei Khimii, 2013, Vol. 83, No. 9, pp. 1409–1413.

Ozone Interaction with Manganese Acetate Solution. Formation of $H_xMnO_2 \cdot nH_2O$ Layers and Microtubes Based on Them

V. P. Tolstoi and L. B. Gulina

St. Petersburg State University, Universitetskii pr. 26, St. Petersburg, 198504 Russia
e-mail: vptol@yandex.ru

Received February 21, 2013

Abstract—We present the first study of Mn(II) cations interaction with ozone fed onto the air/aqueous manganese acetate solution boundary. In the reaction, the layer of $H_xMnO_2 \cdot nH_2O$ of birnessite structure has been formed at the surface. Subsequent ~1–3 μm thick layers drying at air has led to their rolling up to form microtubes with diameter of 20–50 μm and up to 10 mm long.

DOI: 10.1134/S1070363213090016

Birnessite $M_xMnO_2 \cdot nH_2O$ (M = H^+, Na^+, K^+ or other single-charged cations), formed of manganese-oxygen polyhedra containing Mn^{3+} and Mn^{4+} cations, is a crystal of layered structure [1, 2]. Birnessite synthesis is of special interest due to variety of its practical applications: ion-exchanging materials [3], electrode materials of chemical power sources [4, 5], precursors of octahedral molecular sieves with tunnel structure [6], etc.

Known methods of the birnessite preparation are as follows: Mn^{2+} salts oxidation with H_2O_2 in the alkaline solutions [3], Mn^{2+} salts oxidation with molecular O_2 bubbled through the solution [7], reduction of $KMnO_4$ in the acidic medium [8], or hydrothermal treatment of the $KMnO_4$–$MnCl_2$ mixture in the concentrated KOH solution [9]. Under hydrothermal conditions, manganese-oxygen compounds form tubular [10–12] or conical [13] structures.

Recently, much attention has been paid to the tubular inorganic structures preparation. In practice, such structures can be applied to fabricate nano-materials bearing a set of important utilitarian properties. The results attained in this direction have been reviewed in several papers [14–17] with the focus on the synthesis conditions and selected properties of nanotubes and microtubes. Inorganic nanotubes and microtubes can be used to fabricate effective sorbents, electrodes of supercapacitors, electrocatalysts and luminophores with novel properties, for drugs incapsulation, etc.

Nanotubular structures can be often prepared via solvothermal or hydrothermal synthesis of the layered crystalline compounds. Under such conditions, separate nanoplanes of those compounds are rolled up into nanotubes [18, 19] also known as nanorolls [20].

Nanotubes and microtubes can be also obtained via synthesis of inorganic thin layers at the walls of the matrix (template) of regular connected porous structure or at the fibrils surface, with subsequent matrix dissolution [21–23].

The nanotubular structures can be also prepared via another procedure: multinanolayer formation at the template surface [24, 25]. Such multilayer contains the layer of support and at least two layers with different mechanical properties. After the support dissolution, the upper layer rolls up to form variety of structures, including nanotubular ones.

In this work we report the first observation of formation of layers with birnessite crystal structure via the chemical reaction of gaseous ozone and manganese(II) cations dissolved in water; those layers formed microtubes when dried at air.

The interaction of manganese salts with ozone bubbled through the solution was studied in [26].

The first experiments on the manganese acetate solution boundary treatment with ozone revealed that the reaction rate sharply increased when the solution

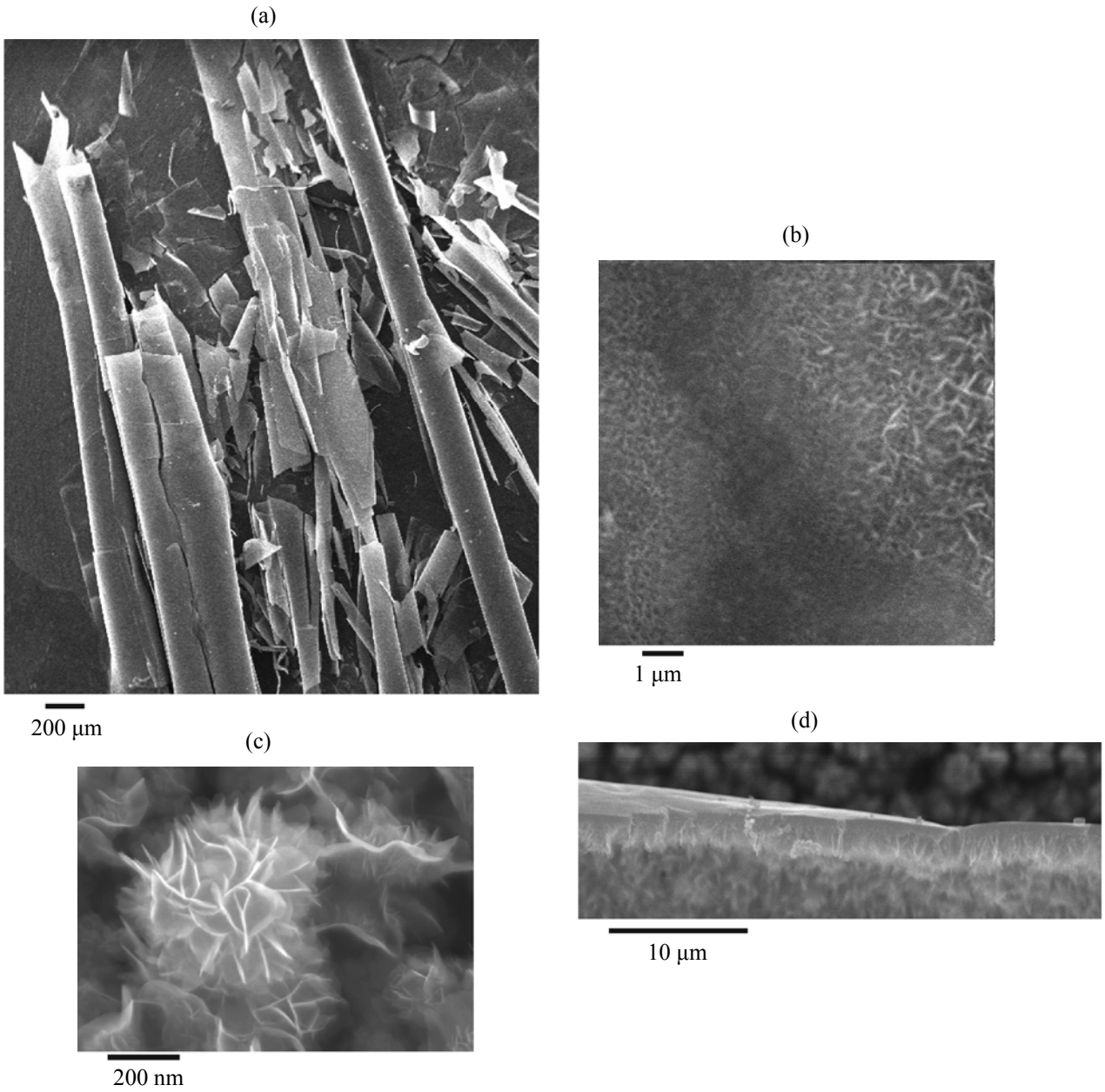

Fig. 1. Microscope pictures of the $H_xMnO_2 \cdot nH_2O$ samples. (a) microtubes general view, (b) the tube outer surface, (c) the tube inner surface, and (d) cross view of the microtube wall.

pH was increased by 0.2 by addition of sodium acetate solution. Under such conditions, after several minutes of treatment with ozone the formation of manganese oxide dark layer was visually observed.

The layers prepared at the interface were transferred onto the crystalline silicon surface and studied by means of optical and scanning electron microscopy. As seen in Fig. 1a, in some cases the microtubes with the diameter of 20–100 μm and up to 10 mm long were observed at the substrate surface. In the case of the sample prepared via 8 minutes treatment with ozone, the microtubes wall thickness was about 3 μm. As the treatment time increased, the layer became thicker (up 10 μm). When the layer thickness was either below 1 μm or above 4 μm, the microtubes were not formed upon drying. Likely, the layers thinner than 1 μm were mechanically too weak

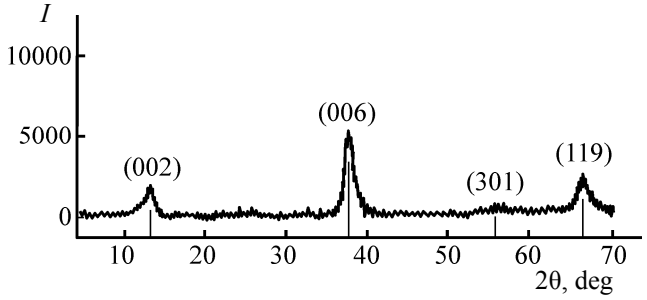

Fig. 2. X-ray diffraction pattern of the $H_xMnO_2 \cdot nH_2O$ layer (5 μm thick) applied onto the silicon monocrystal.

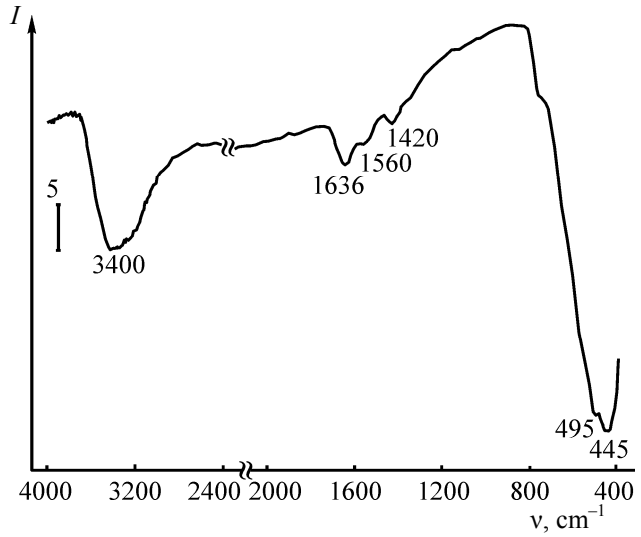

Fig. 3. Fourier IR spectrum of the $H_xMnO_2 \cdot nH_2O$ layer (5 μm thick) applied onto the silicon monocrystal.

to form the stable tube; on the contrary, the layers thicker than 4 μm were likely too stiff to roll up.

Microscope pictures (Fig. 1b) showed that the layer was formed by a set of nanoplanes that were primarily oriented perpendicularly to the interphase boundary, and their packing density was higher at the air side than that at the solution side (Fig. 1c). Importantly, those nanoplanes thickness (as determined from the pictures taken with 150000x magnification) was about 5 nm, and their area was more than 0.1 μm^2.

X-ray spectral microanalysis of the microtubes walls revealed that they were composed of Mn and O atoms; however, in the single spots Na atoms were found, their quantity being at the method detection limit. X-ray diffraction studies (Fig. 2) pointed at the crystalline structure of the layer-forming nanoparticles, namely, that of layered manganese oxide, birnessite $H_xMnO_2 \cdot nH_2O$ [27].

Those results were confirmed by IR spectroscopy (Fig. 3): in the spectrum the bands at 500 and 445 cm^{-1} were observed, assigned to Mn–O bonds [28]. The bands at 3400 and 1630 cm^{-1} in the same spectrum were assigned to water O–H bonds stretching and deformation bands, respectively.

When the $Mn(CH_3COO)_2$ solution surface was treated with ozone admixed to air, Mn^{2+}_{aq} were oxidized by ozone molecules to form Mn(III) [29], then those species partially disproportionated into Mn(IV) in the form of insoluble $H_xMnO_2 \cdot nH_2O$ crystals and Mn(II) cations in the solution.

$$Mn^{2+}_{aq} + O_3 > MnOOH,$$

$$MnOOH > H_xMnO_2 \cdot nH_2O + Mn^{2+}_{aq}.$$

As the oxidation reaction proceeded in the solution containing acetate ions, they likely were adsorbed onto the $H_xMnO_2 \cdot nH_2O$ surface thus preventing crystal growth along one of the axes and leading to the nanoplanes formation instead of ordinary 3-dimensional birnessite crystals.

It might be assumed that at the initial stages of the reaction $H_xMnO_2 \cdot nH_2O$ nanolayers oriented along the air/solution interface were formed. As further nanolayers were formed, the repulsion between them increased, and the layers were aligned primarily perpendicularly to the interphase boundary.

Microtubes formation could be explained as follows: during drying of the layer with gradient of birnessite nanoplanes concentration along the layer thickness, in the bottom part, with lower nanoplanes

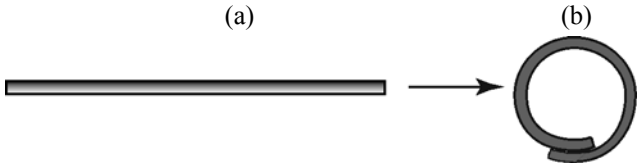

Fig. 4. Suggested model of the microtubes formation upon drying. (a) the sample after synthesis at the solution-air boundary and washing the excess solution off with distilled water, (b) the sample after drying at air. In the picture (a) the density gradient along the direction perpendicular to the layer plane is shown with grey shade gradient.

density, the contractive forces should have appeared due to hydrogen bonds between the nanoplanes, and thus the planar layer geometry should have turned into the tubular one (Fig. 4). Thus, the interface layer separating the solution and the birnessite layer was located in the inner part of the microtube. The mentioned density gradient apparently appeared due to diffuse restriction of ozone interaction with manganese cations in the surface layer of the solution.

Thus, ozone treatment of $Mn(CH_3COO)_2$ aqueous solution surface led to formation of the $H_xMnO_2 \cdot nH_2O$ hydrophobic layer. That layer consisted of the birnessite nanolayers oriented primarily perpendicularly to the interphase boundary; the nanolayers packing density varied along the layer thickness, decreasing towards the solution side. Air-drying of the 1–3 μm layers deposited onto silicon surface gave microtubes with diameter of 20–50 μm and up to 10 mm long. The microtubes were formed likely due to the attractive forces induced by water removal between the nanolayers at the less densely packed surface side of the layer.

EXPERIMENTAL

The electron microscopy pictures were obtained with EVO-40EP scanning electron microscope (LaB_6 cathode, accelerating voltage of 20 keV). The composition of prepared layers was determined with Oxford INCA 350 energy dispersive analysis system equipped with 30 mm^2 Si(Li) detector. FT-IR spectra were recorded using Perkin–Elmer 1760X spectrophotometer (40 scans). X-ray diffraction patterns were obtained with MiniFlex II diffractometer (CuK_α radiation).

Salts $Mn(CH_3COO)_2 \cdot nH_2O$ and $NaCH_3COO$ (Vekton, Russia) were of chemical pure grade. The solutions of $Mn(CH_3COO)_2 \cdot nH_2O$ (0.01 mol l^{-1}) and CH_3COONa (0.02 mol l^{-1}), 2 ml of both, were poured into the 1×1.5×3 cm vessel that was placed into the glass flow reactor (diameter of 2.5 cm, 20 cm long). The air-ozone mixture was supplied from one of the reactor sides, with the rate of 50 ml min^{-1}; ozone was generated with the OZ-1M barrier impulse system (1 g of ozone per hour). The treatment time was 1 to 15 min. After the treatment with ozone, light-brown film was formed at the solution surface was carefully transferred onto the distilled water surface using a specially constructed polyethylene digging bucket. After 10–15 min incubation, the layer was similarly transferred onto the monocrystalline silicon surface, dried, and studied by means of IR spectroscopy, SEM, X-Ray spectral microanalysis, and X-Ray diffraction.

ACKNOWLEDGMENTS

Authors are grateful to A.R. Izatulina (SPSU) for diffraction patterns recording.

The work was financially supported by the Russian Foundation for Basic Research (no. 12-03-00805-a).

REFERENCES

1. Portehault, D., Cassaignon, S., Baudrin, E., and Jolivet, J.-P., *Chem. Mater.*, 2008, vol. 20, p. 6140.
2. Gao, Q., Giraldo, O., Tong, W., and Suib, S. L., *Chem. Mater.*, 2001, vol. 13, p. 778.
3. Prieto, O., Arco, M.D., and Rives V., *J. Mater. Sci.*, 2003, vol. 38, p. 2815.
4. Machefaux, E., Verbaere, A., and Guyomard, D., *J. Power Sources*, 2006, vol. 157, p. 443.
5. Athouel, L., Moser, F., Dugas, R., Crosnier, O., Belanger, D., and Brousse, T., *J. Phys. Chem. (C),* 2008, vol. 112, no. 18, p. 7270.
6. Feng, Q., Yamasaki, K., Yanagisawa, K., and Ooi, K., *J. Mater. Sci. Lett.*, 1996, vol. 15, p. 963.
7. Jun, C., Jia, L., and Suib, S.L., *Chem. Mater.*, 2002, vol. 14, p. 2071.
8. Cheney, M.A., Bhowmik, P.K., Moriuchi, S., Villalobos, M., Qian, S., and Joo, S.W., *J. Nanomater.*, 2008, Article ID 168716.
9. Liu, Z., Ma, R., Ebina, Y., Takada, K., and Sasaki, T., *Chem. Mater.*, 2007, vol. 19, p. 6504.
10. Mao-Wen, X., Guo-Yu, G., Wen-Jia, Zh., Kai-Feng, Zh., and Hu-Lin, L., *J. Power Sources*, 2008, vol. 175, p. 217.
11. Luo, J., Zhu, H.T., Fan, H.M., Liang, J.K., Shi, H.L. and Rao, G.H., *J. Appl. Phys.*, 2009, vol. 105, p. 093925.
12. Wei, X., Hui, X., Fuh, J.Y.H., and Li, L., *J. Power Sources*, 2009, vol. 193, p. 935.
13. Lili, L., Ying, Ch., Yang, L., and Lihong, D., *Mat Let.*, 2007, vol. 61, p. 1609.
14. Patzke, G.R., Krumeich, F., and Nesper, R., *Angew. Chem. Int. Ed.*, 2002, vol. 41, p. 2446.
15. Tenne, R. and Rao, C.N.R., *Phil. Trans. R. Soc. L. A.*, 2004, vol. 362, p. 2099.
16. Fan, H.J., Gzele, U., and Zacharias, M., *Small*, 2007, vol. 3, p. 1660.
17. Gaoshan, H. and Yongfeng, M., *Adv. Mater.,* 2012, vol. 24, p. 2517.
18. Luo, J., Zhu, H.T., Zhang, F., Liang, J.K., Rao, G.H., and Li, J.B., *J. Appl. Phys.*, 2009, vol. 105, p. 093925.
19. Chivilikhin, S.A., Popov, I.Yu., Svitenkov, A.I., Chivilikhin, D.S., and Gusarov, V.V., *Doklady Phys.*, 2009, vol. 54, no. 11, pp. 491–493.

20. Kobayashi, Y., Hata, H., Salama, M., and Mallouk, T.E., *Nano Lett.*, 2007, vol. 7, p. 2142.
21. Jun-Yan, G., Shi-Rui, G., Hai-Sheng, Q., Wei-Hong, X., and Shu-Hong, Yu., *J. Mater. Chem.*, 2009, vol. 19, p. 1037.
22. Bae, C., Yoo, H., Kim, S., Lee, K., Kim, J., Sung, M.M., and Shin, H., *Chem. Mater.*, 2008, vol. 20, p. 756.
23. Shen, G., Bando, Y., and Golberg, D., *Int. J. Nanotechnol.*, 2007, vol. 4, p. 730.
24. Prinz, V.Ya., *Microelectr. Engineer.,* 2003, vol. 69, p. 466.
25. Prinz, V.Ya., *Phys. Stat. Solids (B)*, 2006, vol. 24, p. 3333.
26. Eiji, H., Masaki, I., Haoshen, Zh., *Nanotechnology*, 2008, vol. 19, p. 395605.
27. De, V.V., Pomerantseva, E.A., Kulova, T.L., Grigorieva, A.V., Skundin, A.M., and Goodilin, E.A., *Mendeleev Commun.*, 2009, vol. 19, p. 187.
28. Naidja, A., Liu, C., and Huang, P.M., *J. Coll. Int. Sci.*, 2002, vol. 251, p. 46.
29. Jacobsen, F., Holcman, J., and Sehested, Kn., *Int. J. Chem. Kinetics,* 1998, vol. 30, no. 3, p. 207.